Deriving and Verifying a General Granular Locomotion Scaling Law

by

Stephen Townsend

Submitted to the Department of Mechanical Engineering
in partial fulfillment of the requirements for the degree of

Bachelor of Science in Mechanical Engineering

at the

MASSACHUSETTS INSTITUTE OF TECHNOLOGY

June 2018

Signature redacted

Author . . . . . .
Department of Mechanical Engineering
May 15, 2018

Signature redacted

Certified by . . . . . .
Ken Kamrin
Associate Professor of Mechanical Engineering
Thesis Supervisor

Signature redacted

Accepted by . . . . . .
Rohit Karnik
Associate Professor of Mechanical Engineering
Undergraduate Officer

Deriving and Verifying a General Granular Locomotion Scaling Law

by

Stephen Townsend

Submitted to the Department of Mechanical Engineering
on May 15, 2018, in partial fulfillment of the
requirements for the degree of
Bachelor of Science in Mechanical Engineering

Abstract

The complexities of granular materials make modeling the interactions between grains and solid intruders, such as a wheel, incredible difficult. Often, modeling these interactions requires discrete particle simulation methods, such as the Discrete Element Method (DEM), a process that is prohibitively computationally intensive for large systems. The difficulty of modeling granular materials has posed great difficulty for design engineers, particularly those interested in granular locomotion, since there is no way to gain predictive insight into the performance of a given granular locomotion system. A granular locomotion scaling law was developed, which instructs how to scale size, mass, and driving parameters in order to relate dynamic behaviors of different locomotors in the same granular media.

For the development of this scaling relationship, a general wheel operating in an ideal Coulombic material was considered. Through dimensional analysis, the system was described as a function of a set of dimensionless numbers which are ratios of the dimensional parameters of the system. From the dimensionless description of the system, a set of scaling families are derived, where each member of a family has the same dimensionless inputs but different dimensional parameters. Then, DEM simulations were used to verify that each member of a given scaling family had the same dimensionless outputs.

The DEM simulations found a high level of agreement between the dimensionless outputs of systems in the same scaling family, demonstrating the predictive power of the granular locomotion scaling law.

Thesis Supervisor: Ken Kamrin
Title: Associate Professor of Mechanical Engineering

Acknowledgments

I would like to sincerely thank many people who have helped make my experiences as an undergraduate so transformative and educational. First, Professor Kamrin, who has been incredibly influential in guiding me through both my research endeavors and my undergraduate coursework. Ken has had a larger impact on my education than anyone at MIT, and I am extremely grateful.

James Slonaker's work with wheel optimization for locomotion in granular beds helped to derive the initial scaling law that we used to lay the groundwork for this project. I would like to thank him for the profound influence he had on this project.

Additionally, I would like to thank Qiong Zhang and Shashank Argawal. Without their knowledge of LAMMPS and willingness to help me learn this research would not have been possible.

Contents

List of Figures

List of Tables

Chapter 1

Introduction

Engineers' understanding of the ways through which bodies interact with granular media is limited by the complexity of the behavior of granular materials [1]. Unlike solids and fluids, the constitutive behavior of a granular material cannot be captured by a single differential equation. Instead, granular materials exhibit the behaviors of both solids and fluids; supporting stress below a yield stress like a solid and then flowing under stresses greater than that yield stress like a fluid.

The inability to accurately model the different behavior modes of granular materials has led to substantial design problems for engineers. While some methods for solving these problems do exist, they are often imperfect or impractical. For example, the discrete element method is incredibly accurate, but the computational cost of modeling each granular particle as its own discrete element is prohibitively high for most engineering systems of interest.

One such engineering system of interest is granular locomotion. While there are many engineering systems that perform granular locomotion, such as off-road vehicles, military tanks and the Mars rover, there is not an effective or predictive model of performance for these systems. Common tools such as the discrete element method cannot effectively manage systems of such vast size.

A scaling relationship for granular locomotion systems would allow engineers to utilize scaling families gain insight into the performance of a wide range of systems from a single experiment. This methodology, which is used today to design complex

systems such as airplanes, would allow engineers to simulate or build and test a smaller, more manageable versions of a particular system, and use these experimental or simulated results to accurately predict the performance of a larger system.

This scaling law was derived and Discrete Element Method (DEM) simulations were used to verify its ability to predict performance. The remainder of this chapter will derive the original scaling law from coulombic plasticity and extend it to other more complex situations. Chapter 2 will explain the simulation methodology for the various cases that were explored. Chapter 3 will examine the results of the simulations and lay the groundwork for future work in the space.

1.1 Deriving The Scaling Laws

This section will derive the various scaling laws used throughout the paper. First, a scaling relationship will be deduced by considering a geometrically general wheel operating in a bed of a coulombic plastic material. This law will be expanded in subsequent sections to allow for operating on an incline slope and operating in a material with a different constitutive relationship.

1.1.1 Coulombic Plasticity

Coulombic plasticity is one of the simplest models for a granular material [2]. An ideal Coulombic material has the yield criterion of:

$$\tau = |P| * \mu \tag{1.1}$$

when $P > 0$, where τ is the local shear stress, P is the packing pressure and μ is the internal coefficient of friction of the material. When $P \leq 0$ the material cannot support shear forces and has yield criterion $\tau = 0$. While this model can be used to predict the entire flow field of the sand, it also provides a basis for a dimensional analysis of a granular locomotion system.

1.1.2 Dimensional Analysis

The inputs to this problem are the wheel's defining parameters and the constitutive parameters of the granular material. A general wheel has dimensionless shape described by a function f, a constant width D into the plane, characteristic length L, and a mass M. Additionally, the wheel will be assigned a rotational velocity ω. For the purposes of this problem we will take the mass to be concentrated on the wheel's axle.

The material parameters of the granular media are the granular material's internal friction coefficient μ, the material's density ρ and μ_w, the coefficient of friction between the wheel's surface and the granular material.

The outputs of interest are power P and velocity V, both of which are functions of time t.

The standard non-dimensionalization of this problem yields the following relationship:

$$\left[\frac{P}{Mg\sqrt{Lg}}, \frac{V}{\sqrt{Lg}}\right] = \mathbf{\Psi}\left(\sqrt{\frac{g}{L}}t, f, \frac{g}{L\omega^2}, \frac{D}{L}, \frac{\rho L^3}{M}, \mu, \mu_w\right) \tag{1.2}$$

This relationship can be further constrained if we assume that the granular activity underneath the wheel is close to invariant in the out of plane dimension. In this scenario, $\mathbf{\Psi}$ is constrained on M and D only through their ratio D/M. This implies that $\mathbf{\Psi}$ depends only on D/L and $\rho L^3/M$ through their product. This simplifies the governing scaling law to:

$$\left[\frac{P}{Mg\sqrt{Lg}}, \frac{V}{\sqrt{Lg}}\right] = \mathbf{\Psi}\left(\sqrt{\frac{g}{L}}t, f, \frac{g}{L\omega^2}, \frac{\rho D L^2}{M}, \mu, \mu_w\right) \tag{1.3}$$

This functional dependence implies the existence of families of scaling relations, or systems with different dimensional inputs but equivalent non-dimensional inputs. The scaling law implies that these families, which have th same dimensionless inputs, will also have the same dimensional outputs ($\frac{P}{Mg\sqrt{Lg}}$ and $\frac{V}{\sqrt{Lg}}$). Therefore, defining these families of scaling relationships is very powerful, as it allows engineers to gain insight into the performance of their final system, such as a full size tank, by testing

or simulating a system of a much more manageable size.

These scaling families can be defined as follows. Consider two experiments each with like wheel shape f over the same grains, one with inputs (g, L, M, D, ω) and another with inputs $(g', L', M', D', \omega')$. If $(g', L', M', D', \omega') = (qg, rL, sM, sr^{-2}D, q^{1/2}r^{-1/2}\omega)$ for any positive scalars q, r, s, then the outputs for the respective simulations will be (P, V) and $(P', V') = (Psq^{3/2}r^{1/2}, Vsq^{1/2}r^{1/2})$. Given these scaling families, it is possible to construct a single experiment or simulation to provide insight into the performance over all other systems in the same family. As a result, a scaled model, or the simulation of a scaled model, could be used to predict the performance of a full size system.

One interesting feature of this scaling relationship is that the resulting scaling families have three free parameters, q, r and s, which is due to the dimensionless nature of the material parameters μ_w and μ. The dimensional analysis of some comparable systems, such as systems involving fluids, have fewer than three free scaling parameters since the material properties have dimensions, imposing additional constraints on the size of the space of scaling families.

1.1.3 Extra-planetary Applications

One additional feature of note is that the scaling relationship has the ability to account for changes in gravity. One of the most requested use cases for a scaling relationship such as this one was for extra-planetary exploration. Designing objects which can drive in the sandy conditions of Mars and the moon has been posed a great challenge for engineers, and months have been wasted (cite(space.com Article)) trying to free the current Mars Rovers from being stuck in the Martian sand.

In addition to the difficulties engineers face designing such systems for operation on Earth, designing a system to operate in Mars requires the understanding of how a different magnitude of gravity will effect the vehicles operation. Since sand's yield criterion is a function of pressure, varying the gravitational field, and there for the stress field the sand experiences as a result of its weight, can have quite an effect on the performance of a vehicle such as the Mars rover. As a result, the effectiveness of

this scaling relationship is an important step forward in the design of extra-planetary vehicles.

1.2 Driving on an Incline

The scaling relationship defined in equation 1.3 can easily be extended to systems operating on an incline slope of granular material. To do so, we define an additional input θ which describes the characteristic angel of the slope. Since θ is dimensionless, the scaling relationship simply becomes:

$$\left[\frac{P}{Mg\sqrt{Lg}}, \frac{V}{\sqrt{Lg}}\right] = \Psi\left(\sqrt{\frac{g}{L}}t, f, \frac{g}{L\omega^2}, \frac{\rho DL^2}{M}, \theta, \mu, \mu_w\right) \tag{1.4}$$

Similarly, the scaling families can easily be extended to experiments on an incline slope of granular material. Consider two wheels, each with like shape, operating on a bed made of the same granular material. If their inputs take the form of (g, L, M, D, ω) and $(g', L', M', D', \omega', \theta') = (qg, rL, sM, sr^{-2}D, q^{1/2}r^{-1/2}\omega, \theta)$ for any positive scalar q, r and s, then their outputs will be (P, V) and $(P', V') = (Psq^{3/2}r^{1/2}, Vsq^{1/2}r^{1/2})$.

1.3 Muddy Terrain

In addition to extending the scaling relationship to systems operating on an incline, the scaling law may also be modified to predict the performance of a system operating on different types of materials. One useful material is a cohesive material that has a characteristic yield stress σ_y in addition to internal frictional coefficient μ_f and a frictional coefficient between the material and the wheel mu_w. This material behaves like cohesive grains, a phenomena that often occurs when a granular material gets wet. The input parameters to this system are the same as in equation 1.1, except for the addition of the yield stress σ_y and the output parameters will remain the same.

The initial standard non-dimensionalization yields the following result:

$$\left[\frac{P}{Mg\sqrt{Lg}}, \frac{V}{\sqrt{Lg}}\right] = \mathbf{\Psi}\left(\sqrt{\frac{g}{L}}t, f, \frac{g}{L\omega^2}, \frac{D}{L}, \frac{\rho L^3}{M}, \frac{\sigma_y L^2}{Mg}, \mu, \mu_w\right) \tag{1.5}$$

As in the sandy case, the non-dimensionalization of the system operating on muddy terrain can be further simplified by assuming that the interactions between the wheel and the ground are close to invariant in the out of plane dimension. In this scenario, both the $\mathbf{\Psi}$ depends on D and M only through their ratio $\frac{D}{M}$. This constraint means that both $\frac{\rho L^3}{M}$ and $\frac{\sigma_y L}{Mg}$ effect $\mathbf{\Psi}$ only through their product with $\frac{D}{L}$. Applying this constraint yields the following simplified scaling relationship

$$\left[\frac{P}{Mg\sqrt{Lg}}, \frac{V}{\sqrt{Lg}}\right] = \mathbf{\Psi}\left(\sqrt{\frac{g}{L}}t, f, \frac{g}{L\omega^2}, \frac{\rho D L^2}{M}, \frac{\sigma_y L D}{Mg}, \mu, \mu_w\right) \tag{1.6}$$

This scaling relationship also implies families of like systems which have different real inputs but the same dimensionless inputs and therefore the same dimensionless outputs. These families can be described as follows. Consider two wheels with the same shape function f operating in a bed of the same material, therefore having the same ρ, σ_y, mu_f and mu_w. If the remaining inputs are (L, M, g, D, ω) and $(L', M', g', D', \omega') = (rL, sM, r^{-1}g, r^{-1}\omega, sr^{-2}D)$ then the two systems belong ot the same scaling family.

Note that these scaling relationships imply that the characteristic length of the granular locomotive and the gravitational acceleration applied to the system must be scaled equivalently. This constraint is a result of the additional dimensional parameter for the muddy material relative to the sandy material; the scaling factor of gravity is no longer a free variable like it was in the previous cases. This additional constraint makes experimentally applying this scaling relationship difficult; in order to change the length either the gravitational acceleration or the material parameters must be accurately controlled.

1.4 Simulation

After deriving the scaling relationships for the various cases of interest, Discrete Element Method (DEM) simulations were run in order to verify the predictive power of the scaling relationships. The DEM software used is Large-scale Atomic/Molecular Massively Parallel Simulator, or LAMMPS [3].

DEM is an excellent verification tool. First, DEM agrees extremely well with experimental findings over a wide range of applications, and is generally considered to be as accurate as running an experiment. Secondly, it is extremely easy to accurately adjust the input parameters inside of a simulation. Parameters such as granular material yield coefficients,and rotational velocity, can all be tuned much more easily inside a DEM simulation than they can in a lab experiment. Perhaps more importantly, DEM offers a way to manipulate the gravitational constant, and understanding how these systems vary with gravity is an important potential application of the scaling relationship. Finally, it is possible to accurately track outputs at the granular level in DEM simulations, which is impossible in the lab. Outputs such as the stresses and strains placed on individual grains, or the power expended by rotating the wheel can be extremely difficult to accurately measure in the lab, but are automatically tracked in a DEM simulation.

The subsequent sections will detail the parameters of the various simulations and then display their results.

Chapter 2

Simulation Methodology

A series of DEM simulations were used to verify the usefulness of all the scaling relationships derived in Chapter 1 over a wide range of input parameters. To perform the DEM simulations we used LAMMPS (cite LAMMPS) a well documented open-source molecular dynamics program. The goal of confirming the scaling relationship for a wide range of system parameters necessitated the simulation of many hypothetical systems.

The methodology for verifying the scaling laws using DEM simulations is as follows. The scaling law implies that two systems with the same dimensionless inputs (but possibly with different dimensional inputs) will have the same dimensionless outputs. Therefore, if two systems with the same dimensionless inputs are chosen, there is a direct and predictable relationship between their outputs. The classes of systems which have the same dimensional inputs, and the relationship between their outputs, are described for each iteration of the scaling law in chapter 1 and a class of such systems is referred to as a scaling family.

Once a DEM simulation has been run for a pair of systems in the same scaling family, the scaling relationship can be verified by comparing the system's dimensionless outputs. If the simulation shows that the two systems have the same dimensionless outputs (we use $(\tilde{P}, \tilde{V}) = (\frac{P}{Mg\sqrt{Lg}}, \frac{V}{\sqrt{Lg}})$ as dimensionless outputs) then the scaling law is considered verified for that pair of systems. This agreement is considered a verification of the scaling law because it demonstrates that one system in the family

may be used to predict the performance of other systems in the same family, enabling the scaling law to be used as a predictive tool for granular locomotion system design.

For all of the simulated scaling families, the shape function f of the wheel and the granular material parameters μ and μ_w from equation 1.3 are held constant. Thus, the outputs $(\tilde{P}, \tilde{V}) = (\frac{P}{Mg\sqrt{Lg}}, \frac{V}{\sqrt{Lg}})$ are a function of $\tilde{\rho} = \frac{g}{L\omega^2}$ and $\tilde{g} = \frac{\rho DL^2}{M}$. For the muddy case simulation, the dimensionless outputs are also a function of an additional input, $\tilde{\sigma}_y = \frac{\sigma_y LD}{Mg}$, in order to account for the cohesiveness of the granular material.

This section will be devoted to describing the setup of these simulations and defining the parameter for the various simulations.

2.1 Initial Set Up

This section will describe the setup of the granular locomotive, or wheel, and granular material in the DEM simulations. With the exception of the muddy case, the setup process is the same for all simulations and includes two parts: the creation of and selection of parameters for the granular bed and the creation of the wheel. The simulation box is has periodic boundaries in the x-direction, the direction the wheel travels, and fixed boundaries in the z and y directions.

2.1.1 Granular Bed

The bed used in the all simulations, except the "Muddy Case", is made of poly-disperse randomly packed and gravitationally loaded grains. The simulation box is a three dimensional box with unit thickness into the page. The spherical grains are initialized on a Cartesian lattice with a grid size of 0.008 meters.

The grains are then assigned a random diameter from a uniform distribution between .00051 meters and .00076 meters. They are then allowed to fall through gravity and settle on a rigid square lattice of sand particles that are fixed above the bottom wall of the simulation box. These grains form the bed of granular material which the wheel interacts with.

The particles in this granular bed interact with the neighboring grains and with the wheel according to a Hookean potential that ignores history effects. The potential between two neighboring particles i and j is defined as

$$F_hk = (k_n\delta \boldsymbol{n}_{ij} - m_{eff}\gamma_n \boldsymbol{v}_n) - (k_t \boldsymbol{\Delta} s_t + m_{eff}\gamma_t \boldsymbol{v}_t) \tag{2.1}$$

where δ is the overlap distance of the two particles, k_n and k_t are elastic constants for normal and tangential contacts respectively, γ_n and γ_t are the damping coefficients for normal and tangential contact respectively, m_eff is the effective mass between two particles, defined below, n_{ij} is the vector between the center of the two particles and $\boldsymbol{v}_j$ and $\boldsymbol{v}_i$ are the velocity vectors of the two particles. The equation for the effective mass of two particles with mass $\mathrm{M}_i and M_j is \mathrm{M}_i M_j \frac{}{M_i+M_j}$. For all of the simulations which use this potential, the parameters used were:

A table of parameters for the trudging case can be found below. The positions,

Table 2.1: Grain Parameters

Parameter hline k_n	Value 16400
k_t	4680
γ_n	.5340
γ_t	0

angular velocities and velocities of the individual particles are updated each timestep through constant NVE integration, or integration where the volume and energy of the system remains constant.

2.1.2 Wheel

To simplify the simulations, all of the granular locomotives we simulated were wheels shaped like rectangular plates with a unit thickness into the plane. The plates were made of granular particles that are fixed together to form a rigid body using the âĂŸfix rigidâĂŹ command in LAMMPS.

The fix rigid command alters the way that LAMMPS treats the particles which compose the wheel. Instead of integrating forces over each particle as described above, LAMMPS defines the force and torque on the rigid body as the sum of the forces and torques on each individual particle contained within that body. As a result, the particles are locked in position relative to one another and the rectangular plate behaves as a perfectly rigid wheel.

The wheel is then assigned a rotational velocity in the y-direction. In order to maintain that constant angular velocity, the torque in that same y-direction is set to zero for the duration of the simulation. In other words, the system applies a power to the wheel that is sufficient to always maintain a constant angular velocity even as it propels itself through the sand.

This general setup methodology is used for all the simulations. The next sections will detail the range of scaled pairs that were simulated and the specific parameters of each simulated system.

2.2 Basic Case

This section will detail the simulations used to verify the original scaling law derived from a granular locomotive operating in an ideal Coulomb material. Since this scaling relationship is the first to be verified this way, it was verified with simulations that covered a wide range of qualitative driving styles. For each driving style, a set of three different wheel systems from the same scaling family was simulated. Each system in this set contained a wheel with a with different mass and characteristic length, different gravitational acceleration and different rotational velocity.

The first, which will be referred to as the 'Walking Case', was the most basic of the driving styles. In this case, the wheel does not penetrate particularly deep into the sand and it is assigned a low rotational velocity. As a result, the wheel appears to walk across the sand.

In the Skipping Case the wheel is assigned a rotational velocity of ten times that of the walking case. As a result, the wheel skips across the sand, completely

leaving the ground during each rotation and throwing the granular material beneath it into the air.

The Trudging Case wheel has a much larger mass than the walking case, and therefore sinks very deep into the bed of sand. This added weight causes the wheel to move slower and carry a large number of grains with it.

For each of the cases, three simulations of separate systems with the same dimensionless inputs were completed, and their dimensionless outputs were compared. Within each case, the systems were distinguished by the size of the wheel, into "Big", "Medium" and "Small". Throughout this paper, each simulated system will be distinguished from the others based on the case it belongs to and the size of the wheel.

2.2.1 Walking

The first set of three systems is the "Walking Case". In the walking case, three separate wheels of different sizes, all from the same scaling family, where simulated.Since they were from the same scaling family, all of the qualitative features of the driving patterns of the wheels remained the same between the different simulations.
The wheels in the walking case have a similar density to the granular material, and as a result they does not sink very deeply into the granular bed. Furthermore, they are assigned relatively low rotational velocities, so they did not kick up granular material behind them as they moved through the sand. Additionally, their low rotational velocities meant that they remained in contact with the granular material throughout the duration of their operation. Many of the qualitative aspects of the walking case are captured in the following output frame, which is from the walking case simulation with the largest wheel:

As you can see, the wheel is able to seemingly walk across the top of the grains. It does not sink very deep into the granular bed, and the granular material is left undisturbed behind it. The following table contains the wheel's parameters of interest for this set of simulations. Contained within it are both the dimensional parameters describing the wheel and the system's non-dimensional parameters $\tilde{\rho} = \frac{g}{L\omega^2}$ and $\tilde{g} = \frac{\rho D L^2}{M}$.

Figure 2-1: A output frame of the large wheel from the 'Walking' Case.

Table 2.2: Table of Parameters for Walking Case

Parameter	Small	Medium	Big
Angular Velocity $[\frac{rad}{s}]$	6.28	10.89	4.44
Gravity $[\frac{kgm}{s^2}]$	9.8	39.2	9.8
Length $[m]$	.0168	.0224	.0336
Mass $[kg]$	.0000127	.0000225	.0000508
Non-Dimensional Density $\tilde{\rho}$	55560	55560	55560
Non-Dimensional Gravity $\tilde{g}$	14.79	14.79	14.79

The important realization is that while the dimensional parameters are the same, the non-dimensional parameters are different. This relationship means that the different systems will all have the same dimensionless outputs, in this case dimensionless power and dimensionless velocity. Therefore, the outputs of one simulation may be used to predict the outputs of the other simulations.

In addition to this case, we ran additional simulations to test that validity of the scaling law held for other scaling families. The remaining cases used simulations with different dimensionless parameters and different qualitative driving styles in order to demonstrate the wide range of systems which follow this scaling relationship.

2.2.2 Skipping

The wheel in the skipping case is assigned a velocity which is ten times higher than the velocity in the walking case. As a result, both the qualitative driving characteristics of the wheel and the wheel's dimensionless parameters are different in the skipping case than they are in the walking case.

In the skipping case, the wheels drastically increased angular velocity causes it to skip across the top of the sand. As it does, it completely loses contact with the granular media during parts of its rotation. Additionally, the wheel kicks up granular particles into the air behind it as it drives, imparting some of its inertia into the sand. Many of these qualitative factors can be seen in the following output frame from the skipping case simulation with the largest wheel:

Figure 2-2: A output frame of the large wheel from the 'Skipping' Case. Note that in this frame the wheel is completely disconnected from the surface of the grains, and has kicked grains behind it into the air.

Many of the qualitative differences in the driving patterns of the walking and skipping cases are evident in this frame. Here, it is clear that the wheel has skipped off of the granular material and into the air. Furthermore, the granular material behind it has been disturbed enough that some of it has been thrown into the air.

These qualitative differences in the simulations are important because it allows for the demonstration of the scope of systems that can be predicted using the scaling relationship. In the skipping case, the simulation will test the scaling law's ability

to account for the inertial effects of imparting a velocity to portions of the granular material. The scaling law's ability to do so will support its use in a wide range of systems.

A table containing the same parameters, this time for the skipping case, may be found below.

Table 2.3: Table of Parameters for Skipping Case

Parameter	Small	Medium	Big
Angular Velocity $[\frac{rad}{s}]$	62.8	108.9	44.4
Gravity $[\frac{kgm}{s^2}]$	9.8	39.2	9.8
Length $[m]$	.0168	.0224	.0336
Mass $[kg]$	.0000127	.0000225	.0000508
Non-Dimensional Density $\tilde{\rho}$	55560	55560	55560
Non-Dimensional Gravity $\tilde{g}$	.1479	.1479	.1479

Once again, the entire set of simulations has the same dimensionless parameters despite having different dimensional parameters. The consistency across dimensionless parameters means that the dimensionless outputs are forced to be the same across the simulations.

2.2.3 Trudging

The final case that used the original scaling relationship is the trudging case. In the trudging case the mass is increased tenfold from the walking case and all other parameters remain the same. This increased mass has many effects on the qualitative driving performance of the wheel.

The most obvious difference in the wheel's performance is that it sank substantially deeper into the sand than the skipping or walking cases did. This depth resulted in a trudge-like pattern of motion for the wheel. Additionally, since the wheel is operating at great depth, the wheel moves substantial amounts of sand as it rotates, resulting in a slow and laborious driving pattern.

Many of these qualitative features are evident here:

Figure 2-3: A output frame of the large wheel from the 'Trudging' Case. Note that it sinks substantially deeper into the granular material than the walking case, and displaces substantially more grains.

This output frame from the trudging case with the largest wheel clearly displays the depth which the wheel sinks to. Additionally, the amount of granular material displaced by the wheel is evident due to the mound of material that has accumulated in front of the wheel (in this case the wheel moves to the left as it drives).

A table of parameters for the trudging case can be found below.

Table 2.4: Table of Parameters for Trudging Case

Parameter	Small	Medium	Big
Angular Velocity $[\frac{rad}{s}]$	6.28	10.89	4.44
Gravity $[\frac{kgm}{s^2}]$	9.8	39.2	9.8
Length $[m]$	.0168	.0224	.0336
Mass $[kg]$	.000127	.000224	.000508
Non-Dimensional Density $\tilde{\rho}$	5556	5556	5556
Non-Dimensional Gravity $\tilde{g}$	14.79	14.79	14.79

2.3 Incline Case

This section explores the simulations used to verify the scaling relationship found in equation 1.4, which has been adapted from equation 1.3 to allow for driving on incline slopes. The simulations in these cases used the same granular material, wheel

and simulation box set up as the simulations in the "Basic" Cases detailed above. However, in these cases gravity was applied at an angle in order to simulate an inclined driving slope.

Throughout these simulations, the simulation parameters were similar to that of the "Walking" Case found above, except that gravity was applied at an angle Θ with respect to the vertical. For each value of Θ, a set of three simulations were run, each with the same wheel sizes as found in the Walking, Trudging and Skipping cases above. This set of three simulations was run for values of Θ from 10° to 17.5° in 2.5 ° increments.

Throughout this set of simulations, the major qualitative difference in driving style between the walking case simulations and the incline case simulations was the difficulty which the wheel had in driving. In the walking case, the wheel was able to easily translate across the top of the grains. In the incline case, the wheel does not sink substantially deeper into the granular bed, but the grains behind the wheel tend to cascade downwards due to the incline. As a result, the wheel moves much less distance per rotation, and also displaces many more grains with it's motion. Since this effect is dynamic, it is difficult to visualize with a single frame, but a frame is provided.

Figure 2-4: A output frame of the medium wheel from the 'Incline' Case.

The amount of material the wheel displaces while it drives is evident from the quantity of material that has built up behind the wheel. A table of parameters for all

of the incline simulations may be found below. Note that these simulations use the walking case parameters and those same parameters are repeated for each iteration at a different angle of incline.

While these parameters are fairly repetitive, it is important to verify the scaling relationship at a variety of inclines, in order to ensure that it is valid for many different driving styles that are induced by varying the incline gradient.

Table 2.5: Table of Parameters for 10° Incline Case

Parameter	Small	Medium	Big
Angular Velocity $[\frac{rad}{s}]$	6.28	10.89	4.44
Gravity $[\frac{kgm}{s^2}]$	9.8	39.2	9.8
Length $[m]$	.0168	.0224	.0336
Mass $[kg]$	.0000127	.0000225	.0000508
Non-Dimensional Density $\tilde{\rho}$	55560	55560	55560
Non-Dimensional Gravity $\tilde{g}$	14.79	14.79	14.79
Incline Angle	10°	10°	10°

Table 2.6: Table of Parameters for 12.5° Incline Case

Parameter	Small	Medium	Big
Angular Velocity $[\frac{rad}{s}]$	6.28	10.89	4.44
Gravity $[\frac{kgm}{s^2}]$	9.8	39.2	9.8
Length $[m]$	.0168	.0224	.0336
Mass $[kg]$	.0000127	.0000225	.0000508
Non-Dimensional Density $\tilde{\rho}$	55560	55560	55560
Non-Dimensional Gravity $\tilde{g}$	14.79	14.79	14.79
Incline Angle	12.5°	12.5°	12.5°

Table 2.7: Table of Parameters for 15° Incline Case

Parameter	Small	Medium	Big
Angular Velocity $[\frac{rad}{s}]$	6.28	10.89	4.44
Gravity $[\frac{kgm}{s^2}]$	9.8	39.2	9.8
Length $[m]$	.0168	.0224	.0336
Mass $[kg]$	.0000127	.0000225	.0000508
Non-Dimensional Density $\tilde{\rho}$	55560	55560	55560
Non-Dimensional Gravity $\tilde{g}$	14.79	14.79	14.79
Incline Angle	15°	15°	15°

Table 2.8: Table of Parameters for 17.5° Incline Case

Parameter	Small	Medium	Big
Angular Velocity $[\frac{rad}{s}]$	6.28	10.89	4.44
Gravity $[\frac{kgm}{s^2}]$	9.8	39.2	9.8
Length $[m]$	.0168	.0224	.0336
Mass $[kg]$	.0000127	.0000225	.0000508
Non-Dimensional Density $\tilde{\rho}$	55560	55560	55560
Non-Dimensional Gravity $\tilde{g}$	14.79	14.79	14.79
Incline Angle	17.5°	17.5°	17.5°

2.4 Muddy Case

The Muddy Case is a series of simulations run to test the scaling law proposed for systems with cohesive grains, which can be seen in Equation 1.6. Since the grain properties are different than that of regular granular material, these simulations used a different potential to govern the interactions between grains.

In order to create the cohesive interaction between granular material, this set of simulations used a superposition of the Hookean granular potentials used in previous simulations as well as a Leonard Jones potential. The Leonard Jones potential is described in equation 2.2.

$$E = 4\epsilon[(\frac{\sigma}{x})^12 - (\frac{\sigma}{x})^6] \tag{2.2}$$

Here, ϵ functions as a stiffness parameter, determining the magnitude of the forces, σ allows for the control of the equilibrium distance between particles, and x is the distance between two neighboring particles. As a result, the Leonard Jones can be tuned to work like a spring, supporting stresses in both directions. Unfortunately, for stability reasons, LAMMPS does not allow for granular particles to be connected with simple elastic spring-like potentials, so the Leonard-Jones potential was chosen as a substitute.

This combination of potentials retains the frictional parameters of the granular

scaling relationship while adding a cohesive element in Leonard-Jones, creating a granular material that closely mimics the behavior of mud or wet sand. For each simulation run for the muddy case, the parameters for the grains potentials are as follows:

Table 2.9: Grain Parameters for a Cohesive Material

Parameter	Value
k_n	16400
k_t	4680
γ_n	.5340
γ_t	0
ϵ	.000000002
σ	.000566

The material governed by these potentials differs from the sand used in the original cases because it is cohesive and can therefore support a greater shear load.

2.4.1 Walking Muddy

The new material property vastly changes the way which the wheel interacts with the granular media. Since the media is cohesive, the wheel needs to apply a substantially greater force to pull the material apart. These differences are apparent in the following output frame from the Big Walking Muddy Wheel case.

The most readily apparent difference between this frame and previous simulations is the way the granular material holds its shape after interacting with the wheel, remaining standing up in a pillar-like shape. Non-cohesive grains would not be able to support themselves in a configuration like this one.

The other wheel and system parameters of the muddy case simulations are included in Table 2.10. Note that there is an additional dimensionless number, $\tilde{\sigma}_y = \frac{\sigma_y LD}{Mg}$, which must be fixed between all simulations in order for them to be from the same scaling family.

The simulation parameters for all of the simulations discussed in this paper

Figure 2-5: An output frame from the big wheel simulation from the muddy case. Note that the new potential between grains allows for the sand to create otherwise impossible formations.

Table 2.10: The table of parameters for the walking muddy case simulations. Includes the additional dimensionless parameter $\tilde{\sigma}_y = \frac{\sigma_y LD}{Mg}$ necessary to complete the scaling relationship for a cohesive mateiral.

Parameter	Medium	Big
Angular Velocity $[\frac{rad}{s}]$	10.89	7.25
Gravity $[\frac{kgm}{s^2}]$	14.75	9.8
Length $[m]$	.0224	.0336
Mass $[kg]$	..0000225	.0000508
Non-Dimensional Density $\tilde{\rho}$	55560	55560
Non-Dimensional Gravity $\tilde{g}$	5.55	5.55
Non-Dimensional Stiffness $\tilde{\sigma}_y$	67.5	67.5

can be in tables above. In the next section, we will explore the simulation data and examine the ability of the scaling law to predict the outcome of the various simulations.

2.4.2 Trudging Muddy

In the Walking Muddy case, the new cohesive granular material had the ability to support additional loads than the material used in the original cases. However, the wheel was the same size, and the stronger material meant that the wheel did not sink as deep into the cohesive material.

Another pair of wheels were simulated order to better capture the effects of making the granular material cohesive. This new, 'trudging muddy' pair of wheels were identical to those above except that they were substantially more massive. This additional mass allowed them to sink deeper into the granular material and instigated a greater amount of interaction between the granular material and the locomotor.

Table 2.11: The table of parameters for the trudging muddy case simulations. Includes the additional dimensionless parameter $\tilde{\sigma}_y = \frac{\sigma_y LD}{Mg}$ necessary to complete the scaling relationship for a cohesive mateiral.

Parameter	Medium	Big
Angular Velocity $[\frac{rad}{s}]$	10.89	7.25
Gravity $[\frac{kgm}{s^2}]$	14.75	9.8
Length $[m]$	.0224	.0336
Mass $[kg]$	..000113	.000254
Non-Dimensional Density $\tilde{\rho}$	55560	55560
Non-Dimensional Gravity $\tilde{g}$	5.55	5.55
Non-Dimensional Stiffness $\tilde{\sigma}_y$	67.5	67.5

The new wheel parameters allowed for much more intrusion into the granular material. An example of the additional depth into the material can be found in figure 2-6.

Figure 2-6: A frame outputted from the trudging muddy simulation. Note that the wheel travels substantially deeper into the cohesive granular material than in the walking case

The more massive wheel is able to penetrate substantially deeper into the

cohesive granular material, and further interaction with the flowing cohesive granular material puts more stress on the scaling law, making the trudging muddy case an excellent test of the scaling law for a granular locomotor in a cohesive granular material.

Chapter 3

Data and Results

The purpose of the simulations detailed in Chapter 2 was to verify that the scaling laws proposed in Chapter 1 could successfully predict the performance of a wide range of different granular locomotion systems. Several sets of simulations were run in order to ensure that the scaling law remained valid for many qualitatively different driving conditions and styles, with the goal of verifying the scaling law's ability to account for a wide range of the unpredictable behavior of a granular material.

This chapter will explore the data from the simulations described in Chapter 2. The scaling law implies that all of the simulations with the same dimensionless inputs will have the same dimensionless outputs. Since all of the simulations for each separate case had the same dimensionless inputs, they should all have the same dimensionless outputs, in this case non-dimensional power and non-dimensional velocity.

So, in this chapter, for each case, plots of non-dimensional power and non-dimensional velocity vs non-dimensional time will be provided. For each case, if the scaling relationship is effective, the non-dimensional outputs should all be the same, and thus the lines should overlap. Therefore, the test of the validity of the scaling law will be the degree to which the non-dimensional outputs of different simulations in a given case agree. If they do, then the scaling law and a single system from a given scaling family will provide information on the performance of every system in that same scaling family.

3.1 Basic Case

The first set of tests that will be discussed is the Basic Case. As was discussed in Chapter 2, the basic case consisted of three tests from each of three separate scaling families of plate shaped wheels operating on a sand-like granular material.

The different scaling families were chosen to highlight different unique properties of granular material that make modeling granular locomotion difficult. The Walking case is the simplest of these cases, chosen to somewhat mimic the way a wheel would interact with a rigid surface. The skipping case was chosen to highlight the scaling law's ability to account for the inertial effects of granular material being sent into motion by the wheel. The Trudging Case was designed to explore the ability of the scaling law to account for wheels sinking deep into the sand and displacing large amounts of material.

3.1.1 Walking Case

The first set of tests, called the Walking Case, produced the following results. In these plots, non-dimensional power, time and velocity are defined as

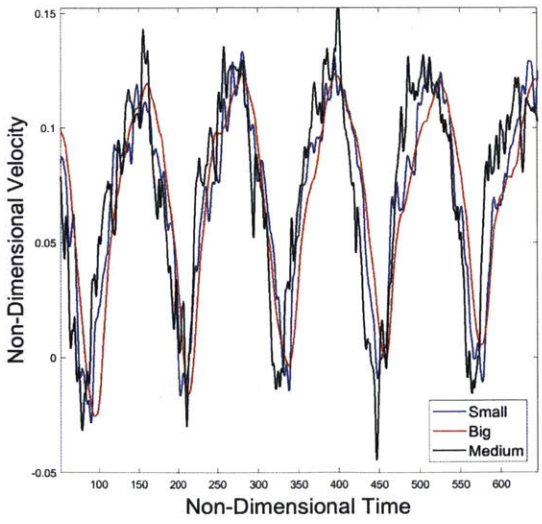

Figure 3-1: Non-Dimensional velocity vs non-dimensional time for the three walking case systems

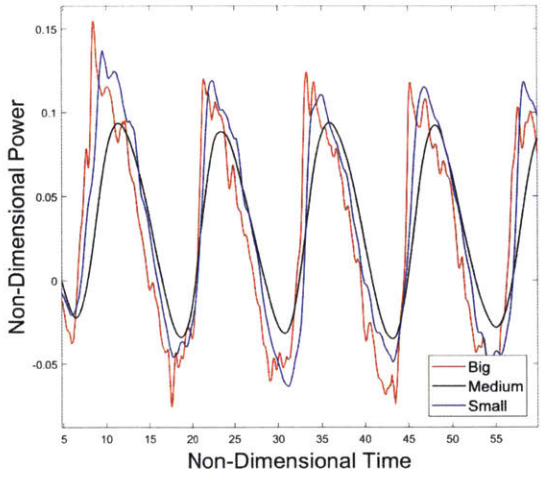

Figure 3-2: Non-dimensional power vs non-dimensional time for the three walking case systems

Its clear that there is good agreement for the walking case. This agreement is unsurprising as in the walking case the granular material interacted with the wheel somewhat like a rigid surface would have; the wheel did not sink very deep and the wheel was unable to displace a substantial amount of material.

3.1.2 Skipping Case

Conversely, in the skipping case, the wheel consistently threw substantial amounts of the granular material behind it into the air as it drove. These inertial effects would not exist if the granular material was a rigid surface, and therefore the scaling law is put under greater stress for these simulations. These plots of non dimensional power and non-dimensional velocity indicate the scaling law's effectiveness in these conditions.

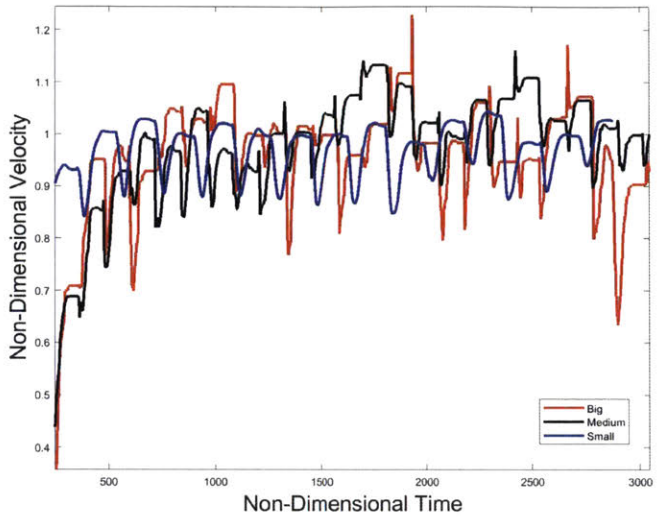

Figure 3-3: Non-Dimensional velocity vs non-dimensional time for the three skipping case systems

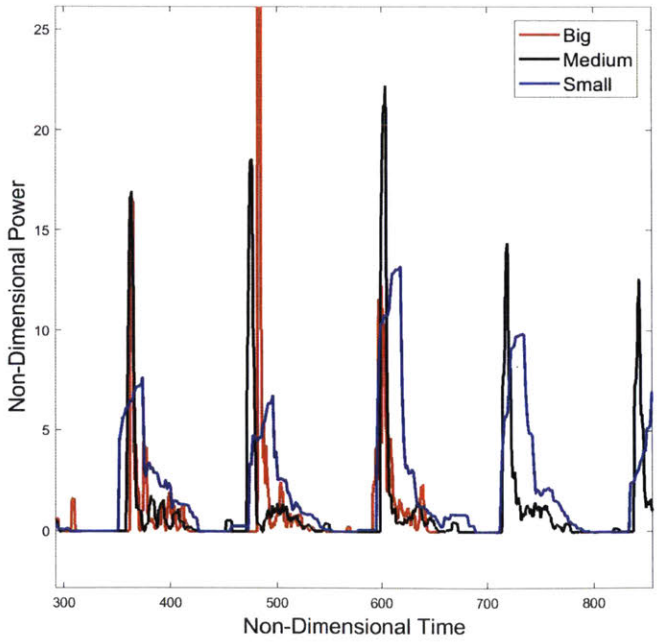

Figure 3-4: Non-dimensional power vs non-dimensional time for the three skipping case systems

In this case the high velocities and powers as well as the non-level surface of the grains leads to a substantially noisier signal for non-dimensional power and velocity. However, while the noisy sections of the plots do not match up perfectly, the scaling law is still extremely effective for capturing the steady state behavior of the non-dimensional power and velocity functions.

The non-dimensional time averaged power and velocities for each of the three wheels operating at steady state are provided in the following table, where $\langle x \rangle$ indicates a time average of x.

Table 3.1: Time Averaged Outputs for the Skipping Case

Parameter	Small	Medium	Big
Non-Dimensional Power $\left\langle \tilde{P} \right\rangle$	1.02	1.09	1.69
Non-Dimensional Velocity $\left\langle \tilde{V} \right\rangle$	.976	.999	.984

Despite some inaccuracy in the prediction of the noise between different simulations, the continuity for the time averaged outputs across these cases suggests that the scaling law is able to accurately predict the steady state behavior of the wheel in each simulation.

3.1.3 Trudging Case

In the trudging case, the wheel's additional mass caused it to sink deep into the granular bed. This added depth resulted in the wheel needing to displace large amounts of granular material during each rotation. The non-dimensional power and velocity plots are below.

The simulations found excellent agreement between the various members of this scaling family, despite the fact that many of the phenomena that make modeling granular materials difficult, such as sinking deep into the sand and displacing lots of material, were extremely prevalent in this case. These results strongly support the validity of the scaling law.

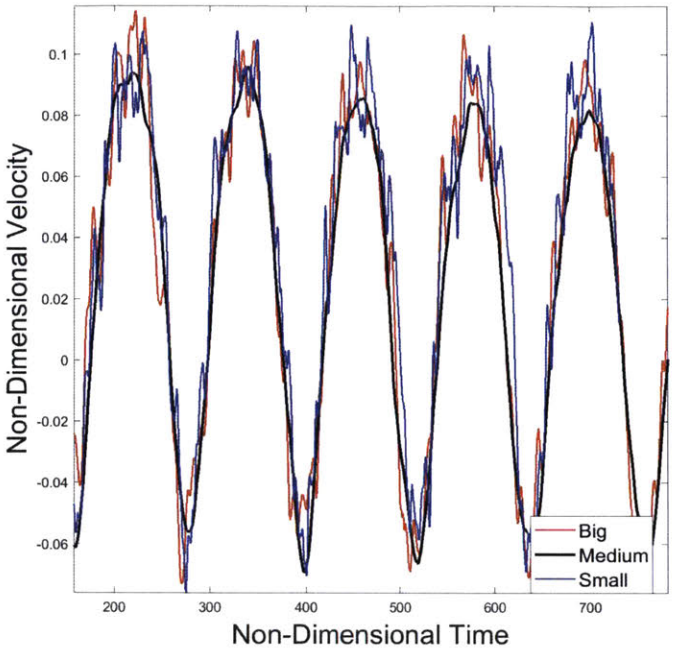

Figure 3-5: Non-Dimensional Velocity vs Non-Dimensional time for the three Trudging Case systems

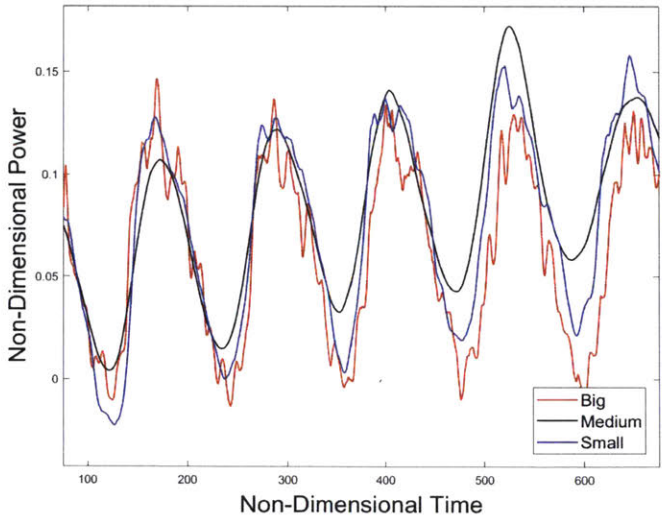

Figure 3-6: Non-Dimensional Power vs Non-Dimensional time for the three Trudging Case systems.

3.2 Incline Case

The Incline Case tested the first hypothesized generalization of the scaling law, driving the wheel up an incline slope of granular material. This generalization added

an additional parameter, Θ, which the dimensionless outputs depended upon. To account for this additional parameter, simulations were run with wheel driving up an incline. For each scaling family three scaled wheels were driven up the same grade of incline slope. The dimensionless outputs of these simulations for incline grades of 12.5 to 17.5 are plotted below.

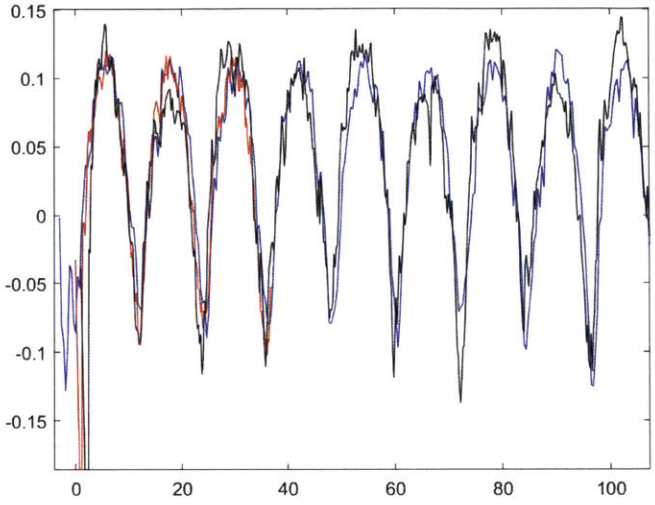

Figure 3-7: Non-Dimensional velocity vs non-dimensional time for the 12.5 incline case. The non-dimensional outputs show excellent agreement.

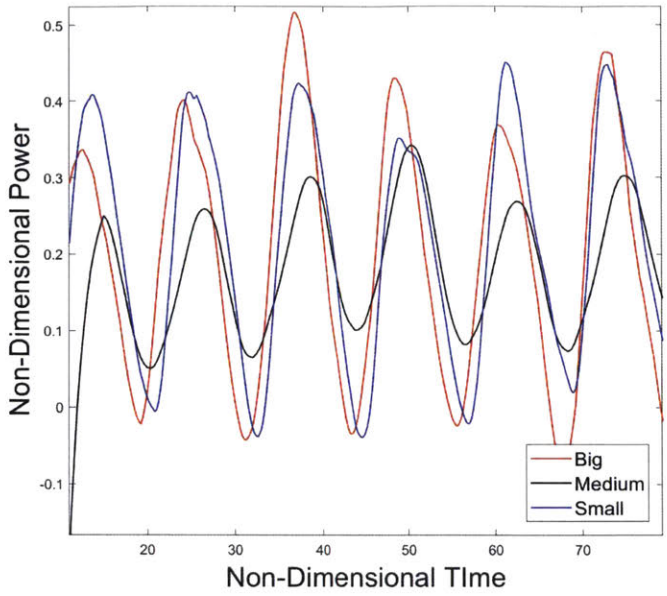

Figure 3-8: Non-Dimensional power vs non-dimensional time for the 12.5 incline case. The non-dimensional outputs show excellent agreement.

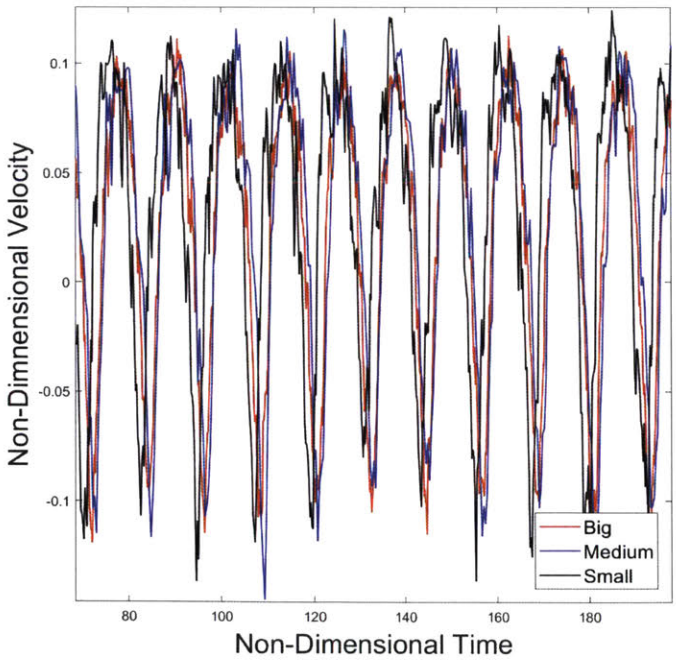

Figure 3-9: Non-Dimensional velocity vs non-dimensional time for the 15 incline case. The non-dimensional outputs show excellent agreement.

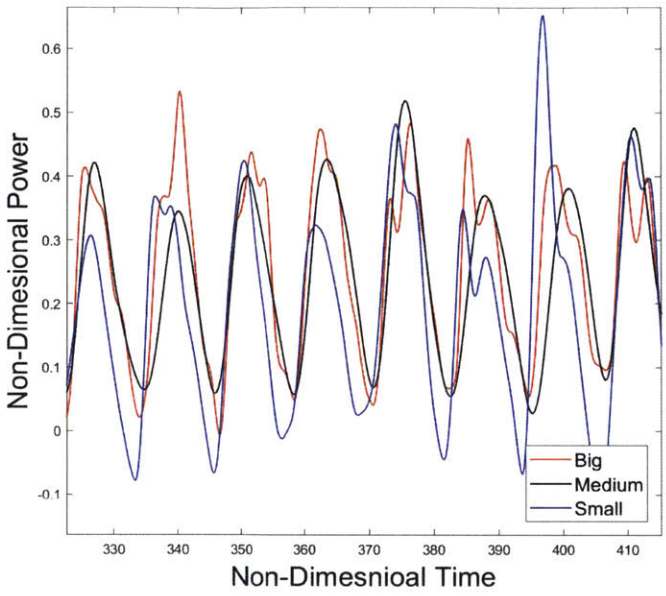

Figure 3-10: Non-Dimensional power vs non-dimensional time for the 15 incline case. The non-dimensional outputs show excellent agreement.

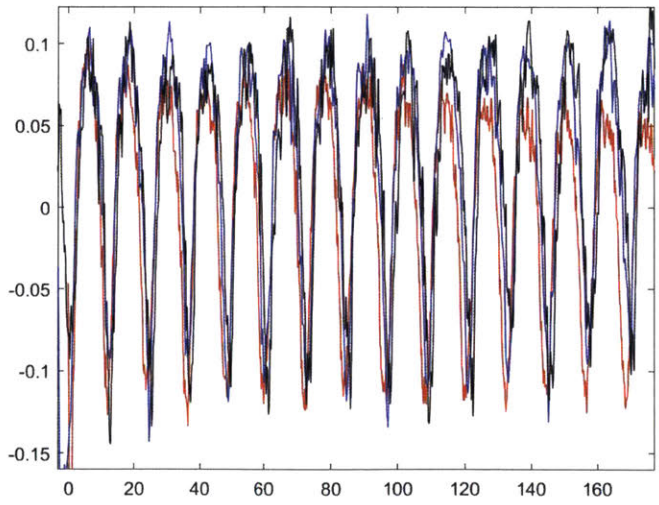

Figure 3-11: Non-Dimensional velocity vs non-dimensional time for the 17.5 incline case. The non-dimensional outputs show excellent agreement.

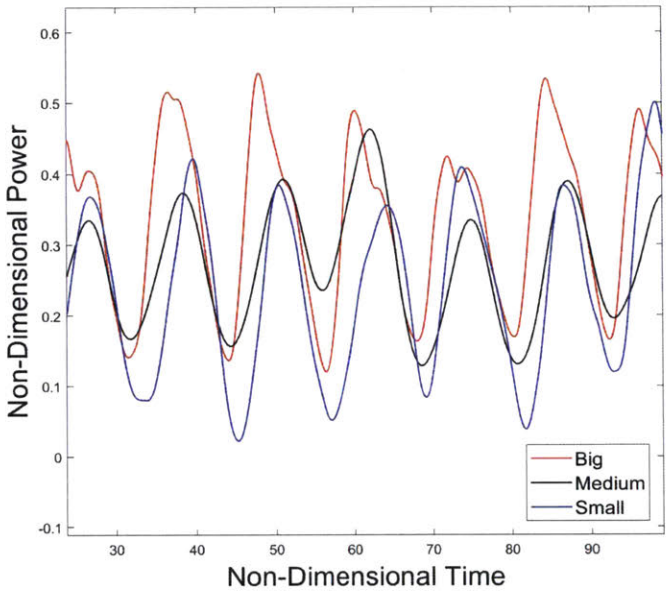

Figure 3-12: Non-Dimensional power vs non-dimensional time for the 17.5 incline case. The non-dimensional outputs show excellent agreement.

The incline simulations show repeatable agreement for a the entire range of incline slopes which were tested. The one exception is the Incline 17.5 case, where the power of the big case stands out as incorrect. In this case, the length scale of the simulation box and the nature of periodic boundaries prevented accurate scaling. The periodic boundaries result in the simulation actually being a series of the same wheels operating on the same slope; there is effectively a wheel operating in front of the wheel seen in the simulation box. In the Big Incline case for 17.5, the length of the simulation box, and therefore the distance between these two wheels, was sufficiently small that the grains displaced and sent downhill by the leading wheel interfered with the driving pattern of the trailing wheel.

Other than interference of the un-scaled length of the simulation boxes in the 17.5 case, the dimensionless outputs of simulations showed excellent agreement, strongly supporting the validity of the scaling law proposed in Equation 1.4.

3.3 Muddy Case

In the Muddy cases the wheel drove over a bed made of cohesive grains that mimic the behavior of mud or wet sand. The additional parameters needed to make the granular material cohesive required the development and application of a new scaling relationship, Equation 1.3. The muddy case simulations test the validity of this new scaling relationship.

For the walking case, the wheel did not sink particularly deep into the grains. As a result, the wheel behaved similar to how it would have had it been on a rigid surface instead of a bed of cohesive grains, and so the excellent scaling results are unsurprising.

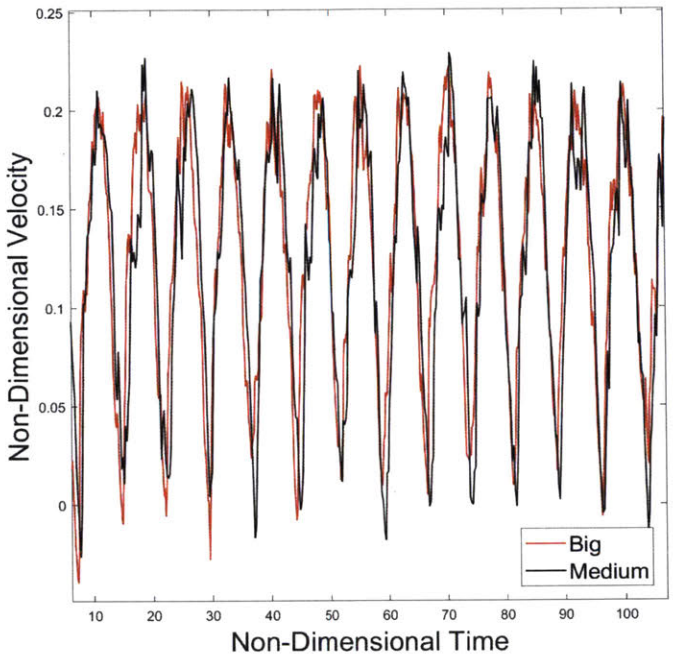

Figure 3-13: Non-Dimensional velocity vs non-dimensional time for the walking muddy case simulations. Excellent agreement between the non-dimensional output of the two simulations

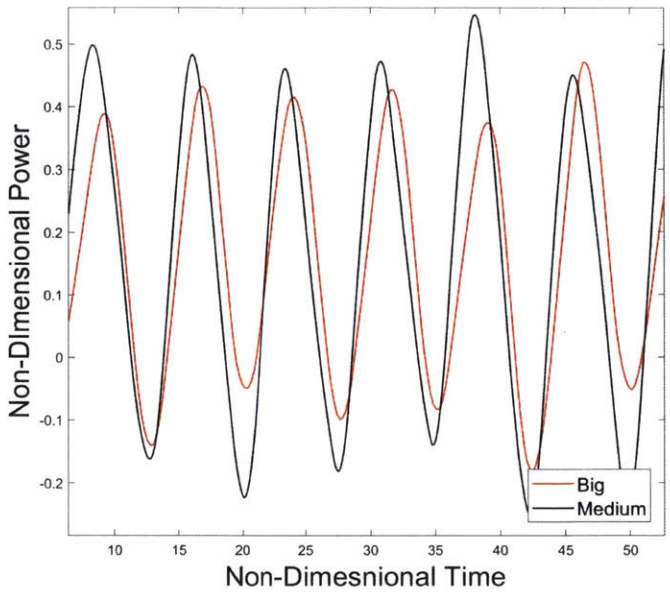

Figure 3-14: Non-Dimensional power vs non-dimensional time for the walking muddy case simulations. Excellent agreement between the non-dimensional output of the two simulations

While the non-dimensional outputs agree, the validation of the muddy scaling law was not considered complete because the wheel and stiff cohesive grains interacted quite rigidly. In the trudging case, the wheels were substantially more massive, and penetrated deep into the granular bed. Consequently, the granular bed did not behave similarly to a rigid bed, but rather like a cohesive bed of grains. The additional interactions between the wheel and the grains give a better indication of the effectiveness of the scaling law for a cohesive granular media.

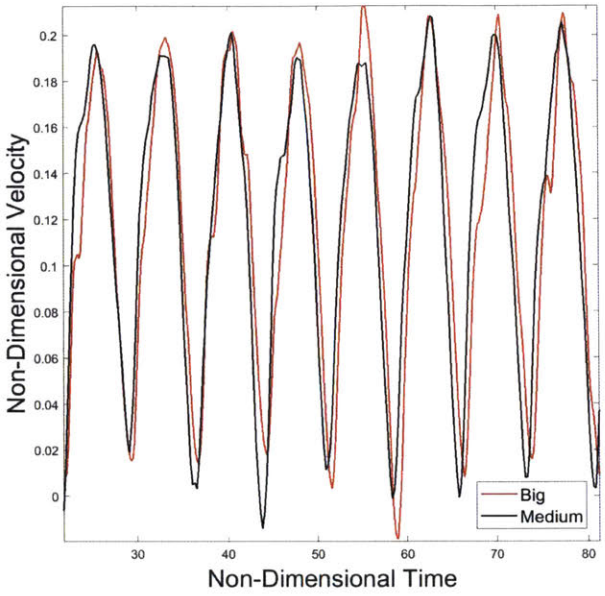

Figure 3-15: Non-dimensional velocity vs non-dimensional time for the muddy trudging case. Notice that, despite the depth to which the wheel sinks, the scaling relationship still finds excellent agreement between the non-dimensional velocities between simulations.

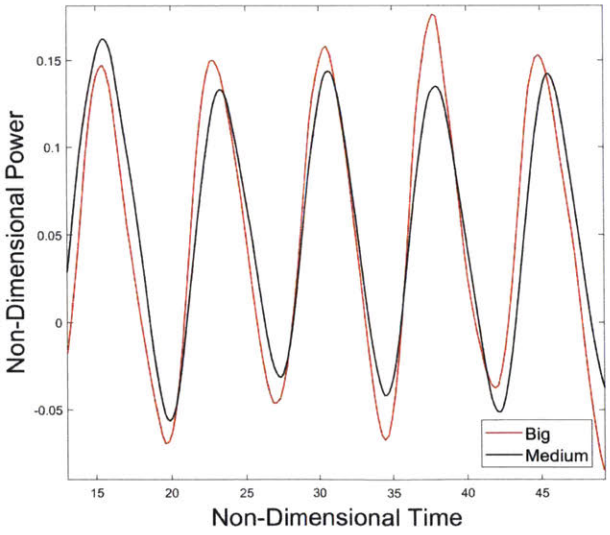

Figure 3-16: Non-Dimensional Power vs Non-Dimensional Time for the muddy trudging case. The non-dimensional outputs for the two simulations in this case show excellent agreement.

Figures 3-16 and 3-15 display the excellent agreement between the non-dimensional outputs of the trudging muddy case. The muddy scaling law in Equation 1.6 is clearly able to account for the additional cohesive interactions between the grains. The ability to account for these interactions in a simple scaling law displays the power of the non-denationalization of granular locomotion systems, and indicates that the scaling law could be further generalized to apply to other granular interaction laws.

3.4 Discussion and Further Experimentation

The scaling law was able to successfully predict the behavior of all of the simulations that were run. It's success is truly impressive when considering the wide variety of parameters, granular materials and driving styles that were tested. Although the simulations run to date are all extremely supportive of the scaling relationship being useful for the design of granular locomotion systems in industry, there is some interesting research that has yet to be done.

One desirable extension of the granular locomotion scaling law is for deformable wheels. In most granular locomotion systems, the wheels of the locomotive deform under the stresses of driving, making this an important inclusion into an effective granular locomotion scaling relationship. It is our goal to eventually show that the scaling law can predict the strain induced in the wheel in addition to predicting the power and velocity outputs of the wheel.

Another necessary advancement of the scaling relationship is the application of it in a three dimensional simulation. Due to time and computational constraints, three dimensional simulations were not run for this project, but displaying the scaling laws functionality in three dimensions is in important step in the scaling law's validation.

Appendix A

Appendix A

A sample input file for the LAMMPS simulation, from the "Biggest Trudging" case:

processors 3 1 3

units si

dimension 3

newton off

boundary p p f

atomstyle sphere

commmodify mode single vel yes

neighbor 0.0005 nsq

variable d equal 0.0008

variable err equal 0.2

variable dl equal d*(1-err)/1.05/(1+err)

variable dh equal d*(1+err)/1.05/(1+err)

variable rho equal 2500

variable latt equal vd*1.0

variable L equal 275

variable q equal 1

variable tau equal $10^{(}-4)/(9.8/d)^{0}.5*1$

timesteptau

lattice sc d

readrestart /home/stownsend/Scaling/HeavyWheel/Biggest/BigWheel1200000.restart

region world block 0 L 0 1 0 200

region sand block 0 L 0 1 0 150

region bed block 0 L 0 1 4 145

region floorregion block 0 L 0 1 0 3

region plateregion block 40 81 0 1 152 157

region plateregioninner block 41 80 0 1 152.5 156.5

createbox 4 world

variable kn equal 2*$10^5 * 3.14/6 * rho * d * d * 9.8 * 10$

$variablektequalkn * 2/7$

$variablegammanequal50 * (9.8/d)^0.5 * 100$

$variablegammatequal50 * (9.8/d)^0.5 * 0$

$pair$style gran/hooke/history kn kt gamman gammat 0.4 1

paircoeff * *

fix 3 all wall/gran kn kt gamman gammat 0.4 1 zplane 0 200

createatoms 2 region bed

label loopb

variable b loop 12400

variable d2 equal random(dl,dh,1)

set atom b diameter d2

next b

jump SELF loopb

createatoms 1 region floorregion

createatoms 3 region plateregion

set type 1 diameter d

set type 1 density rho

set type 2 density rho

set type 3 diameter .0008

set type 3 density rho

set type 4 diameter .0008

```
set type 4 density 10374.62
group wheel region plateregion
group center region plateregioninner
group bottom region floorregion
group grain subtract all wheel bottom
set group bottom type 1
set group wheel type 3
set group center type 4
neighmodify exclude type 3 1
neighmodify exclude type 4 1
neighmodify exclude type 4 4
neighmodify exclude type 3 4
neighmodify exclude type 3 3
neighmodify exclude type 1 1
group plate type 3 4
    velocity grain create 1E14 4928459
    fix 1 wheel move rotate 60.5 0.5 74.5 0 1 0 1.414
fix grav1 grain gravity 9.8 vector 0 0 -1
fix grav2 wheel gravity 9.8 vector 0 0 -1
fix integrate grain nve/sphere

variable cmx equal xcm(plate,x)
variable cmy equal xcm(plate,y)
variable cmz equal xcm(plate,z)
variable wx equal omega(plate,x)
variable wy equal omega(plate,y)
variable wz equal omega(plate,z)
variable tx equal torque(plate,x)
variable ty equal torque(plate,y)
variable tz equal torque(plate,z)
```

```
variable vmx equal vcm(plate,x)
variable vmy equal vcm(plate,y)
variable vmz equal vcm(plate,z)
    compute stress all stress/atom NULL pair
run 1
balance 1.05 shift z 10 1.05
    unfix 1
fix wheelspinning wheel rigid single force * on on on torque * off off off
fix zeroyforce wheel setforce NULL 0 NULL
    dump dump1 all image 100000 /home/stownsend/Scaling/HeavyWheel/Biggest/BigWheel*.jpg
type diameter size 1280 720 center s 0.5 0.3 0.4 zoom 3.3 view 90 90
dump d3 all custom 100000 /home/stownsend/Scaling/HeavyWheel/Biggest/BigWheel*.txt
id type x y z vx vy vz diameter cstress[1] cstress[2] cstress[3] cstress[4] cstress[5]
cstress[6]
dumpmodify d3 format "
restart 100000 /home/stownsend/Scaling/HeavyWheel/Biggest/BigWheel*.restart
    thermo 10000
thermostyle custom step vcmx vcmy vcmz vvmx vvmy vvmz vwx vwy vwz vtx vty
vtz
    run 19
run 180
    label loopa
variable a loop 1500
run 20000
next a
jump SELF loopa
```

Bibliography

[1] Goddard, Joe D. "Continuum modeling of granular media" Applied Mechanics Reviews 66.5 (2014): 050801. Web

[2] Nedderman, RM. "Statics and Kinematics of Granular Materials Cambridge univ" Press, Cambridge (1992). Web.

[3] Plimpton, S. "Fast Parallel Algorithms for Short-Range Molecular Dynamics", J Comp Phys, 117, 1-19 (1995).